Science of the Total Environment 951 (2024) 175646

Contents lists available at ScienceDirect

Science of the Total Environment

journal homepage: www.elsevier.com/locate/scitotenv

The impact of methylparaben and chlorine on the architecture of *Stenotrophomonas maltophilia* biofilms

Ana Rita Pereira [a,b,*], Liam M. Rooney [c], Inês B. Gomes [a,b], Manuel Simões [a,b], Gail McConnell [c]

[a] LEPABE - Laboratory for Process Engineering, Environment, Biotechnology and Energy, Faculty of Engineering, University of Porto, Rua Dr. Roberto Frias, 4200-465 Porto, Portugal
[b] ALiCE - Associate Laboratory in Chemical Engineering, Faculty of Engineering, University of Porto, Rua Dr. Roberto Frias, 4200-465 Porto, Portugal
[c] Strathclyde Institute of Pharmacy and Biomedical Sciences, University of Strathclyde, 161 Cathedral Street, Glasgow G4 0RE, UK

HIGHLIGHTS

- *S. maltophilia* biofilm architecture is possible to evaluate using the Mesolens.
- MP at 15 mg/L increased the complexity of colony biofilms internal structures.
- MP at 15 μg/L and 15 mg/L altered the internal structure and lipid distribution in biomass.
- MP and chlorine together significantly decreased biofilm roundness.
- Biofilm architecture changes reflect adaptative mechanisms to environmental stress.

GRAPHICAL ABSTRACT

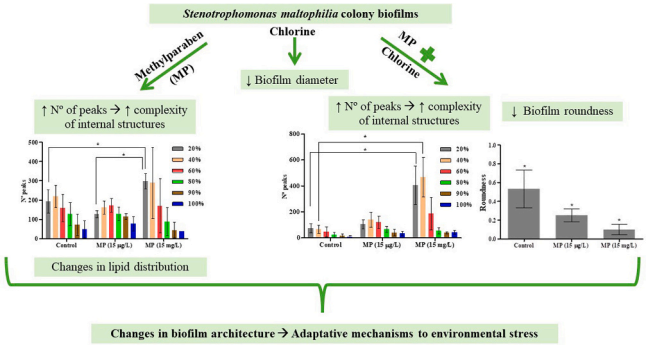

ARTICLE INFO

Editor: Damià Barceló

Keywords:
Biofilm architecture
Chlorine
Colony biofilms
Lipids
Methylparaben
Mesoscopy

ABSTRACT

The biofilm architecture is significantly influenced by external environmental conditions. Biofilms grown on drinking water distribution systems (DWDS) are exposed to environmental contaminants, including parabens, and disinfection strategies, such as chlorine. Although changes in biofilm density and culturability from chemical exposure are widely reported, little is known about the effects of parabens and chlorine on biofilm morphology and architecture. This is the first study evaluating architectural changes in *Stenotrophomonas maltophilia* colony biofilms (representatives of bacterial communities presented in DWDS) induced by the exposure to methylparaben (MP) at environmental (15 μg/L) and in-use (15 mg/L) concentrations, and chlorine at 5 mg/L, using widefield epi-fluorescence mesoscopy with Mesolens. The GFP fluorescence of colony biofilms allowed the visualization of internal structures and Nile Red fluorescence permitted the inspection of the distribution of lipids. Our data show that exposure to MP triggers physiological and morphological adaptation in mature colony biofilms by increasing the complexity of internal structures, which may confer protection to embedded cells from external chemical molecules. These architectural modifications include changes in lipid distribution as an adaptive response to MP exposure. Although chlorine exposure affected colony biofilm diameter and architecture, the colony roundness was completely affected by the simultaneous presence of MP and chlorine. This work

* Corresponding author at: LEPABE - Laboratory for Process Engineering, Environment, Biotechnology and Energy, Faculty of Engineering, University of Porto, Rua Dr. Roberto Frias, 4200-465 Porto, Portugal.
E-mail address: up201505436@edu.fe.up.pt (A.R. Pereira).

https://doi.org/10.1016/j.scitotenv.2024.175646
Received 25 June 2024; Received in revised form 30 July 2024; Accepted 17 August 2024
Available online 20 August 2024

is pioneer in using Mesolens to highlight the risks of exposure to emerging environmental contaminants (MP), by affecting the architecture of biofilms formed by drinking water (DW) bacteria, even when combined with routine disinfection strategies.

1. Introduction

Drinking water distribution systems (DWDS) consist of reservoirs, pipes, and treatment facilities used to deliver water to the consumers. These systems harbour biofilms, which constitute over 95 % of the biomass present within them (Flemming et al., 2002). Biofilms, as organized microbial communities embedded under extracellular polymeric substances (EPS) and attached to biotic or abiotic surfaces (Flemming et al., 2016), are 1000 times more tolerant to stressful environmental conditions or biocides in comparison with planktonic counterparts (Dubois-Brissonnet et al., 2016).

Biofilms are responsible for influencing different factors affecting the quality and safety of drinking water (DW) increasing microbial cell numbers in the bulk phase and causing changes in the organoleptic properties of the water, which can significantly impact human health (Chaves Simões and Simões, 2013). Nevertheless, DW is also affected by exposure to environmental contaminants including parabens (Pereira et al., 2023b). The involvement of parabens in the disruption of endocrine activity (Wei et al., 2021) has raised significant concern pertaining to their toxicological safety profile in DW; these molecules are extensively used as preservatives in daily routine products including personal care products, cosmetics, pharmaceuticals, and food products (Nowak et al., 2018). As a result of the widespread use of parabens in domestic products, aquatic environmental contamination is common, and parabens are routinely detected in DWDS. Therefore, biofilms present in DWDS can be constantly exposed to parabens, altering their characteristics and behavior. Our previous works suggested that exposure to parabens at environmental concentrations may cause modifications on biofilm cell proliferation and matrix composition in comparison to non-exposed counterparts (Pereira et al., 2023a). For instance, DW 7-days-old single and dual-species biofilms composed of *Acinetobacter calcoaceticus* and *Stenotrophomonas maltophilia* revealed increased biofilm cell density and culturability when growing in the presence of methylparaben (MP) at 150 ng/L (Pereira et al., 2023a). Moreover, bacteria exposed to MP also revealed increased virulence and tolerance to disinfection (Pereira and Gomes, 2024). These biofilm adaptations to MP exposure were also accompanied by changes in biofilm conformation and thickness (Pereira et al., 2023a; Pereira and Gomes, 2024). Moreover, EPS composition was also altered by the exposure to MP, specifically in terms of polysaccharides and protein content (Pereira et al., 2023a).

The study of the architecture of biofilms is crucial to understanding how these microbial communities grow and adapt to environmental conditions and become more tolerant to growth control strategies. So far, no study exists to evaluate the impact of parabens on biofilm architecture. In this study, the Mesolens was used to image macro-colony biofilms of *S. maltophilia*, with and without exposure to MP at 15 μg/L (a representative environmental concentration) (Pereira et al., 2023b) and a concentration 1000 times higher (15 mg/L), representative of concentrations encountered in commercially available products containing parabens (in-use concentration) (European Commission (EU), 2014, 2011).

S. maltophilia is an opportunistic pathogen that can be found in DWDS worldwide, being critical for people with weakened immune systems, and is the causative agent of several outbreaks (Brooke, 2021). The presence of *S. maltophilia* in DW (Simões et al., 2007) and their intrinsic antimicrobial resistance (Alawi et al., 2024; Tsvetanova et al., 2022) is a global concern due to its proliferation in DWDS. Moreover, its presence in hospital DWDS has also been linked to hospital-acquired infections (Auld et al., 2023).

The Mesolens is an optical mesoscope that enables sub-micron resolution across multi-millimeter size live biofilms, allowing a greater area of visualization concerning other microscopes (McConnell et al., 2016). Although two studies used the Mesolens to asses colony biofilm architecture (Bottura et al., 2022; Rooney et al., 2020), the present study is the first one evaluating the internal architecture of mature biofilms from a DW bacterial strain, with and without exposure to MP, as well as the spatial organization of lipids, which are an important component of biofilms involved in the initial adhesion and in the structure stability (Conrad et al., 2003). Moreover, the effects of 5 mg/L chlorine (the maximum allowable concentration in DW according to the World Health Organization - WHO) (WHO, 2017), with and without MP exposure, on the colony biofilms architecture were also assessed for the first time using the Mesolens. Chlorination is typically applied in DWDS to control microbial biofilm growth and safeguard DW quality and, consequently, the overall health of DW consumers (Butterfield et al., 2002).

This study extends previous works (Pereira et al., 2023a; Pereira and Gomes, 2024) by offering a timely and unique understanding of the architectural changes on DW *S. maltophilia* biofilms due to MP and chlorine exposure at relevant biological and ecological concentrations (Pereira et al., 2023b). The findings from the study emphasize the importance of considering emerging contaminants in the management of DWDS, including in water disinfection strategies since their presence may impact the biofilm architecture. These modifications may have an impact on biofilm virulence and potentially impact the health of DW consumers.

2. Materials and methods

2.1. Bacteria and culture conditions

Stenotrophomonas maltophilia UV74-sfGFP (*S. maltophilia-gfp*) kindly provided by Uwe Mamat from Cellular Microbiology, Priority Research Area Infections, Research Center Borstel, Leibniz Lung Center, Borstel, Germany was utilized in this study. This strain carries a mini-Tn*7*T-Gm^{R}-P$_{c}$-*sf*GFP_opt element downstream of the *glmS* gene, facilitating the expression of Green Fluorescent Protein (GFP) (Mamat et al., 2023). Bacteria were cultured overnight at 30 °C, under orbital agitation (200 rpm) in R2A broth medium composed of 0.5 g/L peptone (Oxoid, Hampshire, England) 0.5 g/L glucose (CHEM-LAB, Zedelgem, Belgium), 0.1 g/L magnesium sulfate heptahydrate (Merck, Darmstadt, Germany), 0.3 g/L sodium pyruvate (Fluka, Steinheim, Germany), 0.5 g/L yeast extract (Merck, Darmstadt, Germany), 0.5 g/L casein hydrolysate (Oxoid, Hampshire, England), 0.5 g/L starch (Sigma, Germany), and 0.4 g/L di potassium phosphate trihydrate (Applichem Panreac, Darmstadt, Germany), supplemented with gentamycin at a concentration of 60 μg/mL to maintain GFP expression.

2.2. Colony biofilms formation

Overnight bacterial cell suspensions of *S. maltophilia-gfp* were diluted into fresh R2A broth until they reached the mid-exponential growth phase. Subsequently, 100 μL of bacterial cell suspension, adjusted to 1 × 10^{4} colony forming units (CFU)/ml, was inoculated onto 10 mm-thick R2A agar (15 % agar – R2A broth composition is detailed in section 2.1) supplemented with gentamicin at 60 μg/mL within 3D-printed imaging chambers. The selected 3D-printed imaging chambers used in this study were designed on AutoCAD (Autodesk, USA) and featured a 120 mm × 100 mm × 12 mm plate with a 60 mm diameter and 10 mm deep well at its centre to accommodate the agar substrate (Bottura et al., 2022;

Rooney et al., 2020). The chambers, made of black acrylonitrile butadiene styrene plastic (FlashForge, Hong Kong), were printed using a FlashForge Dreamer 3D printer (FlashForge, Hong Kong). Chambers were sterilized with a 70 % (*v*/v) ethanol solution, and then under 405 nm UV light exposure for 20 min before the formation of colony biofilms. Colony biofilms were then incubated at 30 °C for 48 h in the dark and in static conditions in a SciQuip Incu-80S incubator at 60 % relative humidity before imaging. Three independent biological replicates were performed for each experiment.

2.3. Methylparaben exposure

Among different parabens, MP was selected to represent the preservatives class that has emerged as environmentally relevant contaminants since it is the most used paraben in personal care products. MP was tested at two different concentrations: 15 μg/L and 15 mg/L. The lowest concentration (15 μg/L) selected is representative of the levels of parabens encountered in water sources/systems such as wastewater treatment plants (WWTP) and surface waters (Pereira et al., 2023b), and 15 mg/L is representative of an in-use concentration of parabens in approved European products (European Commission (EU), 2014, 2011).

For MP exposure at both concentrations, bacteria were grown overnight as previously described in section 2.2 in R2A broth supplemented with MP at a final concentration of 15 μg/L and 15 mg/L. After that, overnight bacterial suspensions adjusted to 1×10^4 CFU/mL were also grown in R2A agar substrate supplement with MP at both concentrations. Controls were made by forming *S. maltophilia* colony biofilms in the absence of MP.

2.4. Chlorine treatment

Both colony biofilms with and without exposure to MP were exposed to calcium hypochlorite (Fisher Scientific) at 5 mg/L of free chlorine, which is the maximum allowed concentration defined by WHO for total chlorine in DW (World Health Organization (WHO), 2017). For that, both bacterial suspensions (1×10^4 CFU/mL) with and without exposure to MP – described in sections 2.2 and 2.3 were grown in R2A agar substrate for 48 h containing free chlorine at a final concentration of 5 mg/L. Controls in the absence of free chlorine were performed in biofilms formed by *S. maltophilia* previously exposed and non-exposed to MP.

2.5. Mesoscopy assessment

2.5.1. Specimen preparation for imaging

For colony imaging purposes, colonies with and without exposure to MP, and chlorine-treated and untreated colonies were submerged in sterile R2A broth as a mounting solution before imaging. A large coverglass was positioned over the central well of the imaging mould (70 × 70 mm, Type 1.5, 0107999098 - Marienfeld, Lauda-Koenigshofen, Germany), and the colonies were subsequently imaged using the Mesolens in widefield mode. At least three independent biological samples for each condition were prepared for imaging, and images were acquired in duplicate.

2.5.2. Widefield epi-fluorescence mesoscopy

The images of colony biofilms with and without exposure to MP and treated and untreated to free chlorine were acquired using Mesolens, which is a custom-made optical microscope combining high numerical aperture (0.47) with low magnification (4×) (McConnell et al., 2016). More technical and specific details of the microscope setup are described in previous works (McConnell et al., 2016; Schniete et al., 2018). For widefield epi-fluorescence Mesolens imaging, GFP fluorescence was excited by a 490 nm LED (pE-4000; CoolLED, UK), and emitted fluorescent light was transmitted through a 540 ± 10 nm bandpass filter before being detected by a VNP-29MC sensor-shifting CCD camera (Vieworks, South Korea). The correction collars for the Mesolens were set to values corresponding to water immersion, and the specimens were imaged with water immersion ($n = 1.33$) to minimize spherical aberration caused by refractive index mismatch (Rooney et al., 2020). Note that, the acquisition parameters were optimized for each experiment to use the full dynamic range of the detector.

2.5.3. Assessment of lipids localization with mesoscopy

To determine lipid localization, colony biofilms with and without exposure to MP, and treated and untreated with free chlorine were grown on R2A agar (as described in section 2.3) and supplemented with Nile Red (NR) (72,485, Sigma-Aldrich, USA) at a final concentration of 5 μg/L supplemented into the agar substrate (Rooney et al., 2020). Colony biofilms were imaged using widefield epi-fluorescence mesoscopy as described before (section 2.4.2) using a 490 nm LED to excite fluorescence from GFP, and an additional 580 nm LED was used to excite fluorescence from NR, with a detection bandwidth of 630 ± 25 nm. Where two-channel imaging was performed, images were acquired sequentially and were saved separately for processing and analysis.

2.6. Image analysis

Widefield epi-fluorescence mesoscopy z-stacks were deconvolved using Huygens Professional version 19.04 (Scientific Volume Imaging, The Netherlands, http://svi.nl) with a Classic Maximum Likelihood Estimation algorithm. A theoretical point spread function tailored to the experimental setup was generated within Huygens Professional. Deconvolution computations were executed on a server running a 64-bit Windows Server 2016 Standard operating system (v.1607), powered by two Intel® Xeon® Silver 4114 CPU processors clocked at 2.20 and 2.19 GHz, with 1.0 TB of installed RAM.

Image analysis was performed using FIJI (Schindelin et al., 2012). The diameter of colonies was determined by segmenting a horizontal line measuring 1 pixel wide from one end of the colony to the other and then using the "Analyse ➔ Measure" function of FIJI. The roundness of colony biofilms, which is a common definition used in digital image processing for characterizing 2-D shapes was determined to understand the effects of chlorine disinfection with the simultaneous presence of MP on biofilm architecture. The roundness was defined according to Eq. 1:

$$\text{Roundness} = \frac{4\pi \times \text{Area}}{\text{Perimeter}^2} \quad (1)$$

Therefore, a roundness value of 1 indicates a perfect circle, while the value decreases towards 0 for highly non-circular shapes. The area and perimeter of colony biofilms were determined using FIJI software. The process involves careful adjustment of thresholds and image processing techniques to ensure accurate delineation and measurement. The detailed methodology used is described in Supplementary Material.

Raw data was used for all measurements, with brightness- and contrast-adjustments made using FIJI for presentation purposes only. To observe the fine structures away from the centre of the colonies, long exposure times were required. Consequently, this sometimes resulted in a slight fluorescence saturation at the colonies' centre. However, this saturation did not obscure the complex structures, allowing fine details to remain visible.

2.6.1. Polar transformation

The intensity profile of bacterial colony biofilms along the radial direction was performed using the FIJI plugin *polar transformer* (Schindelin et al., 2012). A schematic image analysis workflow is described in Fig. 1. This plugin performed an image transformation from polar to Cartesian coordinates (A). Then, vertical line selections were taken at different positions (20, 40, 60, 80, 90, and 100 %) on the polar-transformed image (B), corresponding to circumferences around the biofilm taken at different radial distances from its centre, which are positioned at a distance from the centre defined by 0.2 × r, 0.4 × r, 0.6

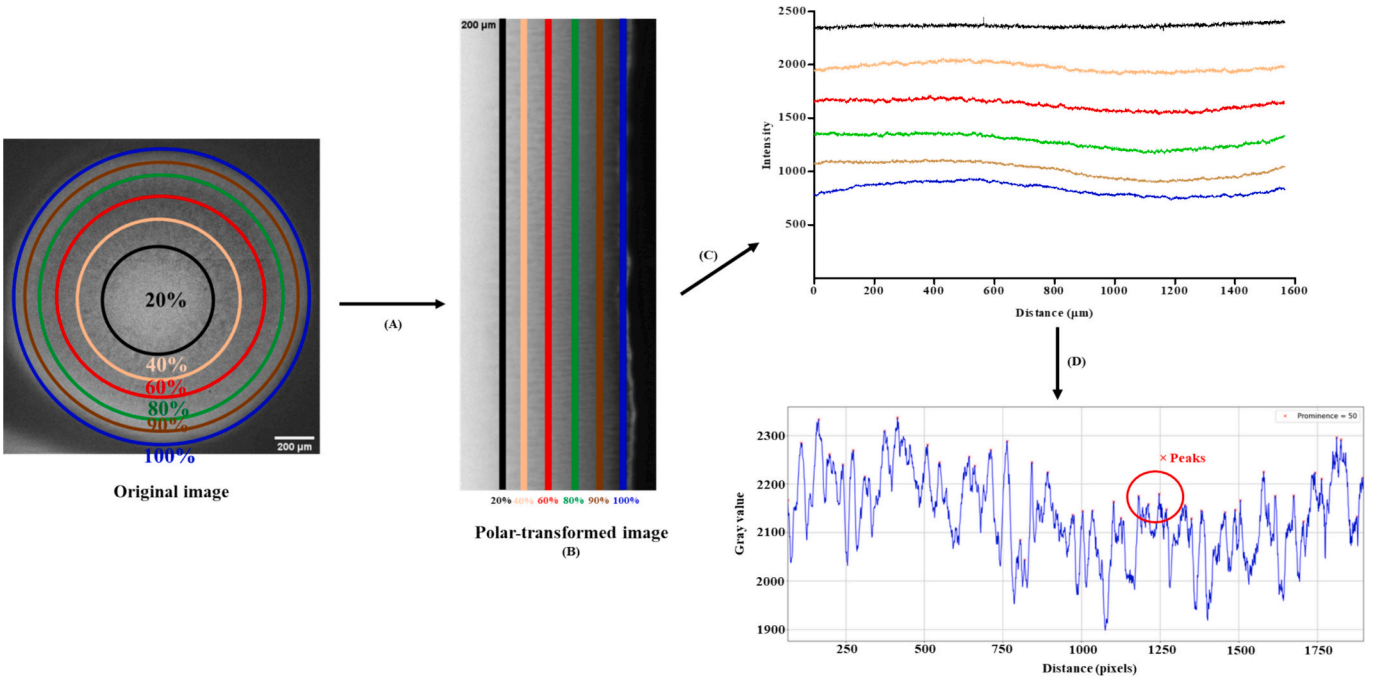

Fig. 1. Image analysis workflow. A widefield Mesolens image is opened on FIJI, and through Polar Transformer FIJI plugin a conversion from polar to Cartesian coordinates was performed (A). Then, vertical line selections were taken at different positions (at a distance from the colony centre of 20, 40, 60, 80, 90, and 100 % of the colony radius) on the polar-transformed image (B) and different signal profiles were plotted around colony biofilm (C) and were exported to Python. Using Python, signal profiles were analysed with a custom script to locate and quantify the peaks (D).

× r, 0.8 × r, 0.9 × r and 1 × r respectively (r is the colony radius) (Fig. 1). Intensity profiles were obtained for each line selection using the *plot profile* feature in FIJI (C). Acquired intensity profile measurements by averaging over a line width of 20 pixels. The number of peaks in each colony biofilm, reflecting the complexity and presence of structures inside these biofilms, was also determined at different radial distances using the *find\peaks()* function with Python (D).

2.6.2. Lipids distribution analysis

The spectral overlap between GFP and NR was mitigated using a difference operation in FIJI to visualise the lipid distribution in colony biofilms. The same polar transformation approach (Section 2.5.1) was applied to obtain the intensity profile of each channel (GFP and NR) for each replicate colony with some modifications. A horizontal line in the middle of polar-transformed image (corresponding to a colony section from its centre until the edge) was selected to plot the intensity profile. In this case, the line width was equal to 200 pixels to the acquired intensity profile measurements. Moreover, since different colonies have different diameters, data obtained was resampled in relation to the colony diameter and normalized.

2.7. Statistical analysis

The experimental data were analysed using the statistical program GraphPad Prism 8.0 for Windows 10 (GraphPad Software, La Jolla California, USA). The mean and standard deviations (SDs) within samples were calculated for all cases. First of all, it was evaluated if the data obtained for each assay followed a normal distribution or not and, consequently, they were classified as parametric or non-parametric using D'Agostino and Pearson omnibus normality test. Then, for parametric data, the differences between measurements were obtained by the application of ANOVA with Tukey's post-test (since comparisons between more than two groups were performed). For nonparametric data (roundness values), Kruskal-Wallis test with Dunnus post-test (for more than two different groups) was also performed. For all the tests performed, statistical calculations were based on a confidence level of ≥95 % ($P < 0.05$ was considered statistically significant).

3. Results

3.1. Impact of MP at environmental and in-use concentrations on colony biofilm architecture

To assess the consequences of MP exposure on colony biofilms architecture, *S. maltophilia-gfp* colony biofilms were grown in the presence and absence of MP at an environmentally relevant concentration (15 µg/L) and an in-use concentration (15 mg/L). Fig. 2 reveals different architecture of colony biofilms with and without exposure to MP, and further differences are observed in colony morphology for the two concentrations of MP applied. In all cases, the centre of colonies comprised a dense cellular mass, but finer structures analogous to channels are visible around the centre of the colony (Fig. 2 – A, B, C). The architecture differences obtained for colony biofilms with and without exposure to MP resulted in different intensity profiles obtained along the radial distance (Supplementary Material – Fig. S1). Indeed, a more constant (flat) intensity profile was obtained for the control specimens, in comparison to colony biofilms with exposure to MP, where intensity profiles were found to have more irregularities (Fig. S1), implying a more intricate architecture. In addition, colony biofilms with exposure to MP at both concentrations revealed higher intensity values at different radial distances in comparison to control (Fig. S1).

Fig. 2-D represents the number of peaks (which reflects the complexity and existence of structures inside the biofilm) obtained for colony biofilms with and without exposure to MP at different radial distances. The number of peaks reflects a pronounced change in the intensity of the GFP signal, which suggests the existence of channel structures. Analysing Fig. 2-D, the number of peaks is generally higher in the centre of the colony until a radial distance of 40 % and then decreases, revealing the existence of few structures on the periphery of the colony.

Overall, it was also found an increasing trend in the number of peaks obtained for colony biofilms with exposure to MP in comparison to the

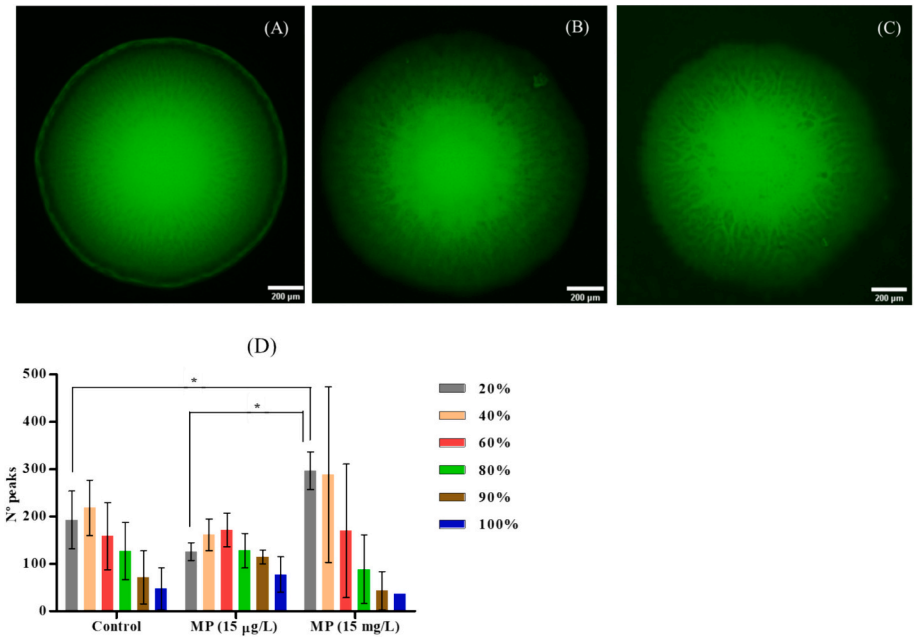

Fig. 2. *S. maltophilia-gfp* colony biofilms without MP - control (A) and with exposure to MP at 15 µg/L (B) and 15 mg/L (C). The number of peaks at different positions (at a distance from the colony centre of 20, 40, 60, 80, 90, and 100 % of the colony radius) was obtained for *S. maltophilia-gfp* colony biofilms without MP (control) and with exposure to MP at 15 µg/L and 15 mg/L presented (D). * - samples were statistically different from each other (ANOVA, post-hoc Tukey's test, $P < 0.05$).

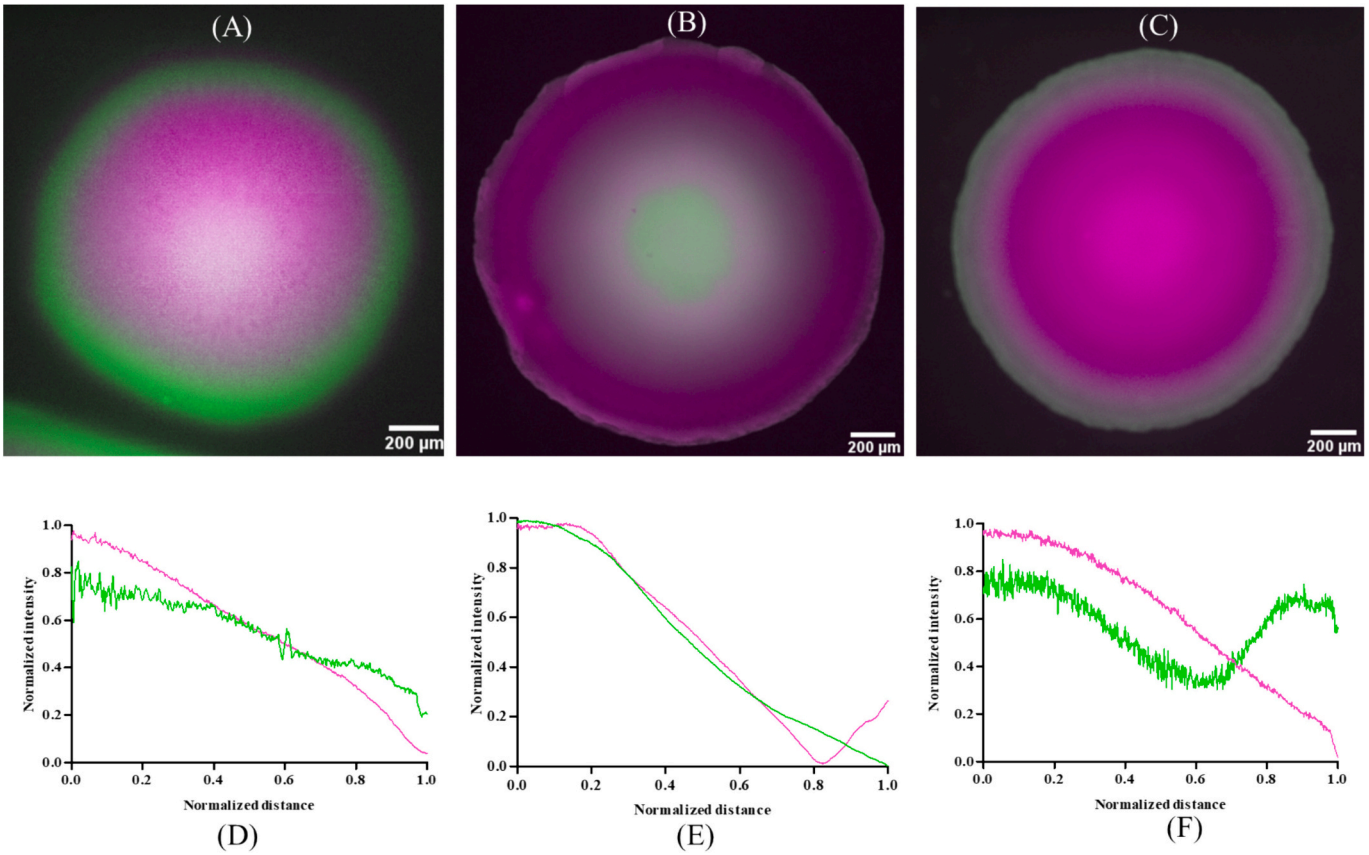

Fig. 3. Spatial distribution of lipids of *S. maltophilia-gfp* colony biofilms without MP - control (A) and with exposure to MP at 15 µg/L (B) and 15 mg/L (C). Cells are shown in green, while Nile Red-stained lipids appear in magenta. Intensity profiles of GFP (in green) and NR (in magenta) channel of *S. maltophilia-gfp* colony biofilms without MP – control (D) and with exposure to MP at 15 µg/L (E) and 15 mg/L (F).

control (Fig. 2-D). This difference in the number of peaks was more pronounced in the centre of the colonies (20 %) when comparing the control with colony biofilms with exposure to MP at 15 mg/L ($P < 0.05$, Fig. 2-D). Indeed, from the peak profile analysis the exposure to MP at 15 mg/L produced biofilms with an average of 297 channel structures at position 20 %, whereas the control (without exposure to MP) only produced biofilms with an average of 193 channel structures ($P < 0.05$).

3.2. Effects of methylparaben on lipids distribution inside colony biofilms

The spatial distribution of lipids was evaluated with NR for colony biofilms with and without exposure to MP at both concentrations. Fig. 3 shows representative *S. maltophilia-gfp* colony biofilms without (A) and with exposure to MP at 15 μg/L (B) and 15 mg/L (C), and their respective intensity profile of both channels (GFP and NR) – D to F. It is possible to see that environmental and in-use concentrations of MP induced changes in the distribution of lipids and cells in *S. maltophilia-gfp* colony biofilms. Colony biofilms without exposure to MP have an increased presence of lipids in the centre of colony (Fig. 3 – A). However, when *S. maltophilia-gfp* colony biofilms are exposed to MP at 15 μg/L, the lipid distribution is altered, and there is an increased presence of lipids on the periphery of the colony (Fig. 3 – B). Curiously, MP-exposed *S. maltophilia-gfp* colony biofilms at 15 mg/L also revealed the distribution of lipids concentrated in the centre of the colony (Fig. 3 – C). Indeed, the results reveals that the intensity of NR, and, therefore, the lipid distribution, decreased linearly along the radius of the colony (Fig. 3 - D, E, F). However, the NR intensity increases from circa of 80 % of radial distance of the colony until the periphery for colony biofilms exposed to MP at 15 μg/L, resulting in the overlapping of NR intensity in relation to GFP intensity (Fig. 3 – E), and, therefore, in the magenta color of the colony periphery (Fig. 3 – B). On the opposite, the intensity profile of GFP also revealed an overlapping of GFP intensity relative to NR intensity in the colony periphery for both colony biofilms without (control) and with exposure to MP at 15 mg/L (Fig. 3 – D and F), resulting in the green color of the colony periphery (Fig. 3 – A and C). These results prove that MP alters the biofilm structure, specifically the distribution of lipid and cells.

3.3. The effects of free chlorine on colony biofilms with and without exposure to MP

To evaluate the effects of free chlorine on colony biofilm architecture, as well as the consequences of MP presence in disinfection effectiveness, colony biofilms with and without exposure to MP were grown with free chlorine at 5 mg/L (Fig. 4).

Modifications in biofilm structure and architecture induced by free chlorine treatment were observed (Fig. 4), with increasing concentrations of MP. Loss of structural integrity of biofilms is visible at the colony periphery when colonies were grown in the presence of 5 mg/L of free chlorine and 15 μg/L of MP (Fig. 4 – B). This effect is amplified when colony biofilms were grown in the presence of free chlorine and MP at 15 mg/L (Fig. 4 – C). Intensity profiles were obtained for free chlorine-treated colony biofilms with and without exposure to MP at both concentrations (Supplementary material - Fig. S2). Although the intensity of the GFP channel decreases along different radial sections (20 % until 100 %) for all conditions tested, free chlorine-treated colony biofilms with exposure to MP at 15 mg/L showed a higher gap between 20 % and 60 % intensity, in comparison to the other conditions (Fig. S2). Moreover, a significant decrease in GFP intensity from the middle of the colony (60 %) until the periphery (100 %) was observed for colony biofilms with MP exposure at 15 mg/L, suggesting a decrease in biofilm cellular density (Fig. S2). However, the number of peaks was much higher for free chlorine-treated colony biofilms grown with MP presence at 15 mg/L ($P < 0.05$) at radial distances of 20 and 40 %, highlighting a statistically significant change in the biofilm architecture when compared to control, even at the centre of the colony biofilm (Fig. 4 - D). This was expected since chlorine non-treated colony biofilms also showed a higher number of peaks than these exposed to 15 mg/L of MP (section 3.1, Fig. 2 – D).

The diameter of colony biofilms was also greatly affected when colony biofilms developed exposed to MP (alone), chlorine (alone), and even in the simultaneous presence of both MP and chlorine. In Fig. 5,

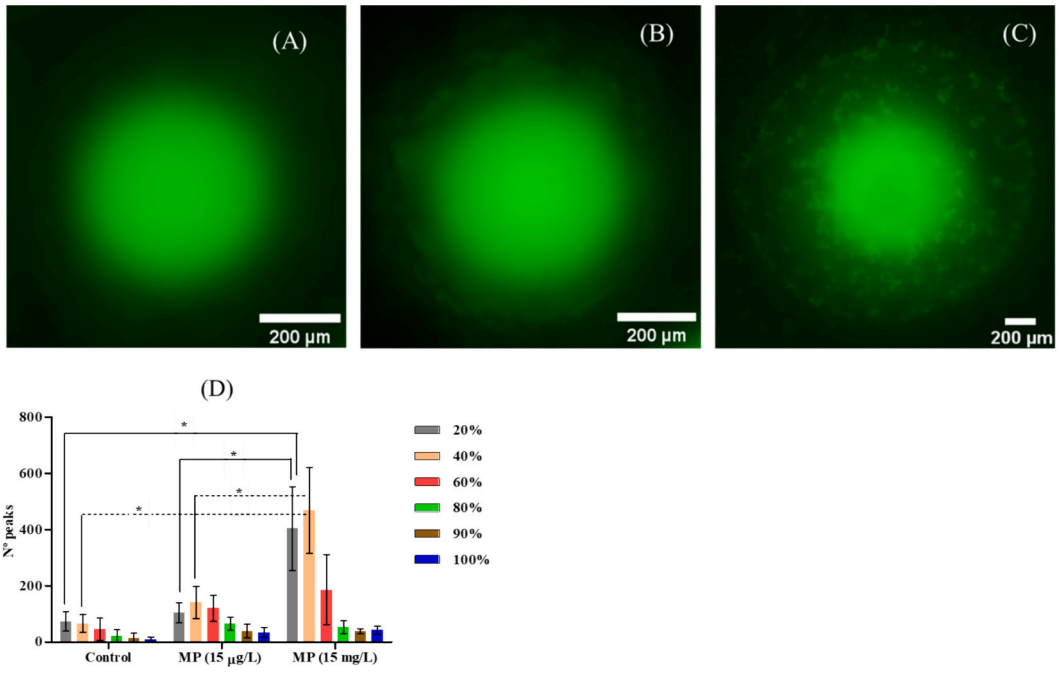

Fig. 4. Free chlorine-treated *S. maltophilia*-gfp colony biofilms without MP – control (A) and with exposure to MP at 15 μg/L (B) and 15 mg/L (C). The number of peaks (at a distance from the colony centre of 20, 40, 60, 80, 90, and 100 % of the colony radius) was obtained for free chlorine-treated *S. maltophilia*-gfp colony biofilms without MP (control) and with exposure to MP at 15 μg/L and 15 mg/L are presented (D). * - samples were statistically different from each other (ANOVA, post-hoc Tukey's test, $P < 0.05$).

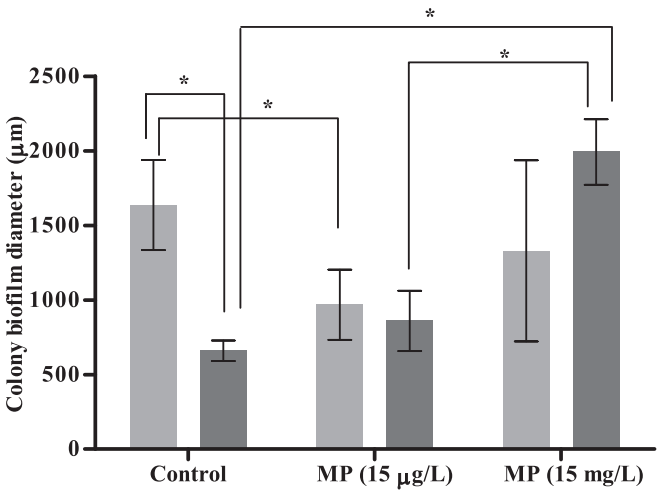

Fig. 5. Diameters (µm) of colony biofilms without (control) and with exposure to MP (at 15 µg/L and 15 mg/L), non-treated (▬) and treated with free chlorine at 5 mg/L (▬). * - samples were statistically different (ANOVA, post-hoc Tukey's test, $P < 0.05$).

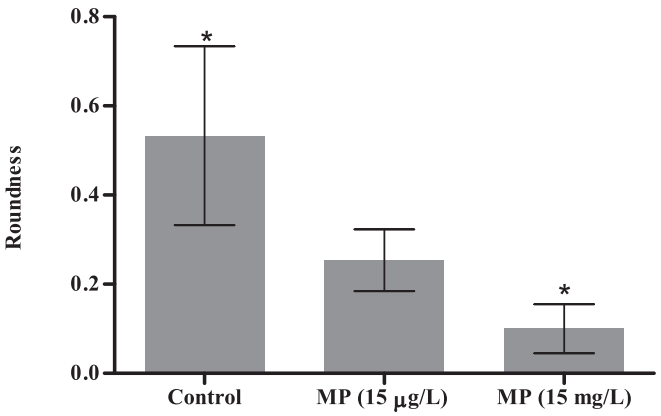

Fig. 6. Roundness of colony biofilms treated with free chlorine at 5 mg/L without (control) and with exposure to MP (at 15 µg/L and 15 mg/L). A roundness value of 1 indicates a perfect circle, while the value decreases towards 0 for highly non-circular shapes. * - samples were statistically different (Kruskal-Wallis, post-hoc Dunnus test, $P < 0.05$).

colonies diameter (µm) of non-treated and free chlorine-treated colony biofilms, with and without exposure to MP at both concentrations are presented.

The presence of MP (alone without chlorine treatment) at the lowest concentration tested (15 µg/L) caused a two-fold decrease in the diameter of colony biofilms in comparison to the non-exposed counterparts ($P < 0.05$). However, this decrease on the colony biofilm diameter was not statistically significant from the MP exposure at the highest concentration tested (15 mg/L) ($P > 0.05$).

The presence of free chlorine at 5 mg/L affects the growth of colonies by decreasing its diameter in comparison to biofilms non-exposed to chlorine. The colony biofilm diameter decreases by three-fold for chlorine-treated biofilms, in comparison to non-treated counterparts ($P < 0.05$) – Fig. 5. While non-treated colony biofilms presented an average diameter of 1636 ± 302 µm, chlorine-treated colony biofilms only showed an average diameter of 659 ± 56 µm (Fig. 5). However, chlorine-treated colony biofilms exposed to MP at 15 mg/L showed increased diameter, in comparison with chlorine-treated colony biofilms non-exposure to MP ($P < 0.05$). This may suggest that the simultaneous presence of MP and free chlorine did not decrease the biofilm colony diameter (Fig. 5). However, it caused disturbances in colony biofilm growth (Fig. 4).

Colony biofilm images representing disinfection treatment were diffuse and the roundness of colonies were found to be affected by the simultaneous presence of chlorine and MP at both concentrations tested. The roundness provides a measure of how close a colony biofilm is to be perfectly circular, with values close to 1 indicating shapes close to a perfect circle (Fig. 6). Results suggested a decrease in colony roundness with exposure to MP from 15 µg/L to 15 mg/L, reflected by lower values of roundness obtained with increasing concentrations of MP. Indeed, colony biofilms treated with free chlorine at 5 mg/L and without exposure to MP (control) revealed a roundness of 0.5 ± 0.2, whereas colony biofilms with exposure to MP at 15 mg/L showed a roundness equal to 0.1 ± 0.04 ($P < 0.05$) – Fig. 6.

4. Discussion

Parabens are emerging environmental contaminants that pose significant concerns regarding their potential to disrupt microbial ecology and dynamics (Liu et al., 2024). Their widespread consumption and continuous discharge lead to ubiquitous distribution in aquatic environments, with concentrations ranging from ng/L to µg/L (Pereira et al., 2023b). Moreover, parabens may accumulate in aquatic environments due to incomplete removal by traditional wastewater treatment processes (Wang et al., 2021). Therefore, microbial communities that inhabit these water systems are constantly exposed to environmental contaminants of emerging concern. Previous studies have already reported differences in biofilm characteristics and behavior induced by the exposure to MP, propylparaben (PP), and butylparaben (BP) individually and in combination, at trace concentrations commonly found in DWDS (Pereira et al., 2023a). These differences suggest changes in biofilm conformation and architecture, with potential implications for bacterial virulence (Pereira et al., 2023a). Bacterial biofilms grown exposed to parabens at environmental concentrations are more virulent and tolerant to water disinfection strategies (Pereira et al., 2023a; Pereira and Gomes, 2024).

This study is the first analysing the impact of MP, as a representative environmental emerging contaminant, on the biofilm architecture and the distribution of key resources, at the mesoscale. For that, *S. maltophilia-gfp* colony biofilms were grown in R2A agar with and without MP at environmentally relevant (15 µg/L) and in-use concentrations (15 mg/L), for 48 h. Both colony biofilms with and without exposure to MP were imaged using the Mesolens to visualise their structure. The distribution of lipids in colony biofilms was also examined. Furthermore, the effects of chlorine treatment, commonly applied in DWDS as a tertiary treatment to control microbial growth and ensure safe drinking water (Gackowska et al., 2016; Lin et al., 2017), on biofilm architecture, were also investigated. Free chlorine-treated biofilms at 5 mg/L were visualised, along with biofilms exposed to both free chlorine and MP at selected concentrations. Results suggest that colony biofilms grown in the presence of MP at both concentrations exhibit different architectural conformations. The presence of MP induced changes in the biofilm structure, as evidenced by the denser centre and the presence of distinct structures such as channels within the colonies. These alterations are reflected in intensity profiles, with MP-exposed colonies showing more irregular profiles when compared to non-exposed counterparts. Moreover, higher intensity values were observed in MP-exposed colony biofilms at an in-use concentration, indicating a potential concentration-dependent effect on the biofilm architecture. Particularly, colony biofilms grown exposed to MP at the highest concentration (15 mg/L) appear to have more pronounced and complex internal structures, as reflected by the higher number of peaks in the intensity profile. These internal structures are known to facilitate the material exchange between biofilms and the external environment (Wilking et al., 2013). More internal structures as channels may be indicative of stressful conditions (nutrient depletion) for bacterial cells

since bacteria never stop to find the optimized method to survive (Wang et al., 2022). Therefore, the presence of MP may induce environmental stress on colony biofilms, changing their architecture and characteristics to adapt to these conditions. A recent study also described modifications of the length and diameter of internal channel structures present in *Escherichia coli* colony biofilms which was elicited by changing nutrient availability and environmental conditions (Bottura et al., 2022).

The colony biofilm diameter of *S. maltophilia-gfp* exposed to MP at 15 μg/L was lower than for the non-exposed counterparts, suggesting a perturbation on bacterial growth induced by MP at environmental concentrations. This corroborates the increase in internal structures inside these colony biofilms exposed to MP as a possible survival strategy.

Previous studies have reported the effects of various environmental contaminants (mainly musks and pharmaceuticals compounds) on the biofilm structure and composition, particularly regarding biofilm thickness and EPS concentration (Arruda et al., 2022; Wang et al., 2019). Cao et al. (2012) also revealed changes in the structural configurations and hydrodynamic properties of the biofilm polymeric matrix, when exposed to contaminants such as uranyl and chromate. However, studies assessing the impact of parabens on biofilm architecture are scarce, particularly regarding biofilms representative of those formed in DWDS. Kenchenten (2017) has already shown that the exposure of *Pseudomonas* sp. biofilms to MP at 1000 ng/L promoted an increase in the biofilm thickness. This effect of increased biofilm thickness induced by MP exposure and different biofilm conformations was also described by Pereira et al. (2023a) regarding single *S. maltophilia* biofilms and *A. calcoaceticus* and *S. maltophilia* dual-species biofilms grown for 7 days with MP presence at 150 ng/L.

The investigation into the influence of MP on colony biofilm architecture also revealed interesting shifts in lipid distribution patterns. Lipids are part of the biofilm matrix (15 % approximately) (Flemming and Wingender, 2010) and generally include phospholipid, glycolipid, neutral lipid, and lipopolysaccharides in 61 %, 21 %, 16 %, and 2 % proportions, respectively (Vandana, 2023). Although lipids are not the main components of the biofilm matrix, it has been demonstrated that they are critical in modulating microbial biofilms (Alim et al., 2018). The presence of lipids in biofilms has a significant role in promoting the adhesion of bacterial cells, biofilm formation, in protecting biofilms from hostile environmental conditions and is also crucial for the stability of the biofilm structure (Conrad et al., 2003). Moreover, lipids are also located in bacterial cell membranes, which are mainly composed of phospholipids, along with proteins and carbohydrates (Barák and Muchová, 2013).

In this study, while non-exposed colony biofilms exhibited a central accumulation of lipids, MP exposure induced redistribution of lipids towards the periphery of the colonies at environmental concentrations, which seems to be also accompanied by a decrease in biofilm cell density. However, at the in-use concentration, lipid distribution reverted to a central accumulation pattern. These observations suggest complex interactions between MP and biofilm. A higher content of lipids on the periphery of the colony may suggest a mechanism of adaptation and protection to environmental stress (Liu et al., 2016). This may also be related to higher stability in the bacterial bilayer and a decrease in membrane fluidity (Benamara et al., 2011). Changes in lipid distribution may consequently have some implications on bacterial metabolic processes, stress response, and the production of virulence factors (Rivera et al., 2022). In addition, it is conceivable that dynamic changes in lipid profiles may also have detrimental effects on bacterial cellular shape and cell physiology (Alim et al., 2018).

Previous works on microbial lipid dynamics within biofilms highlight the importance of lipid distribution in biofilm formation and stability (Flasiński et al., 2016, 2018). Flasiński et al. (2018) evaluated the interactions of parabens with bacterial membrane lipids and their affinity for monolayers, suggesting that parabens (MP, ethylparaben – EP, PP, and BP) interact with these membrane lipids, affecting surface film modification and potentially influencing biofilm hydrophobicity and structural integrity. These modifications include the fluidization of lipid monolayers and were more pronounced for more hydrophobic parabens (BP) since the affinity of this compound for the lipid environment is the highest (Flasiński et al., 2018). A previous study also revealed the collapse of bacterial monolayer induced by BP exposure (Flasiński et al., 2016).

Biofilm control in DWDS is mainly achieved with chemical disinfection, in particular using chlorine since it affects biofilm formation at every stage of development (Chen and Stewart, 2000). Chlorine can reduce microbial growth rate and cause the detachment of cells from biofilms (Chen and Stewart, 2000). However, there is no study to date reporting a complete inhibition of biofilm growth (Butterfield et al., 2002). This may be explained by the slow penetration of chlorine into biofilms, with chlorine neutralization by the organic matter in the surface layers of biofilms occurring faster than its diffusion into the biofilm interior (Stewart et al., 2001).

Regarding the effect of chlorine treatment on the architecture of colony biofilms, free chlorine-treated colony biofilms without MP presence were smaller (more than half) in diameter when compared to their non-treated and non-exposed to MP counterparts. Therefore, chlorine disinfection significantly affected the bacterial growth of biofilms. Moreover, the simultaneous presence of chlorine and MP (in particular at 15 mg/L) seems to cause a higher perturbation on colony biofilm architecture, revealing more irregularities and a decrease in biofilm cells density. The roundness of free chlorine-treated colony biofilms was also significantly affected by the presence of MP showing a direct response to the increase of the paraben concentration. Colony biofilms grown simultaneously with the presence of MP and chlorine shown to be more irregular than free chlorine-treated colony biofilms without exposure to MP, suggesting pronounced repercussions on the biofilm architecture. This interaction between MP and free chlorine may result in public health implications since it has a pronounced effect on the biofilm architecture which can result in bacteria with increased virulence and tolerance to disinfectants (Stanton et al., 2022). However, more studies should be performed regarding this issue. Indeed, the formation of disinfection by-products (DBPs) may also occur (Li and Mitch, 2018) from the interaction between MP and free chlorine, which may be able to cause more pronounced modifications in the biofilm architecture. In fact, parabens containing a hydroxyl group are highly reactive molecules with chlorine, resulting in electrophilic aromatic substitution reactions and the consequent formation of halogenated parabens (Postigo et al., 2021). Halogenated parabens are known to have more negative effects on humans and aquatic organisms, compromising ecosystems and public health (Postigo et al., 2021). Overall, understanding the architecture and dynamics of colony biofilms representative of those grown in DWDS with constant exposure to environmental contaminants of emerging concern (MP) and chlorine treatment can help in the prediction and mitigation of possible ecological and public health implications.

5. Limitations and suggestions for future research

Although the present study provides pioneer insights into the impact of parabens, particularly MP, on the architecture of biofilms formed by an *S. maltophilia* strain isolated from DW, these biofilms found in DWDS can contain a diversity of bacteria. However, by strategically selecting a limited number of bacterial species, one can optimize the use of resources and efforts to obtain robust, consistent, and meaningful results about the impact of MP and chlorine in the biofilm structure. These findings provide crucial evidence that trace levels of MP in the environment can significantly alter the biofilm architecture, showcasing the adaptability of these structures to environmental changes. Notably, MP also affected how biofilms respond to chlorine disinfection, which could pose a serious public health risk and significant concern for DW management organizations. Future studies can build on the present findings

by investigating the impact of MP on additional bacterial species and exploring a wider range of microbial interactions. Expanding research to include complex microbial communities in controlled environments that simulate DWDS can provide a wider perspective on the impact of MP in DW biofilms and their tolerance to disinfection. Such scientific data can contribute to the development of more effective management and treatment strategies to eliminate and/or reduce the presence of MP and control microbial load in DW, reducing the threat they represent to the environment and public health.

6. Conclusion

This study demonstrates the significant impact of MP and chlorine on microbial biofilm architecture, particularly *S. maltophilia-gfp* colony biofilms. The results highlight the importance of understanding the effects of emerging environmental contaminants on microbial communities in aquatic environments where these compounds are increasingly prevalent. Different architectural modifications in colony biofilms with exposure to MP suggested a concentration-dependent effect on biofilm structure. Notably, MP exposure led to a denser centre and the formation of discernible internal structures within colonies, and a decrease in the diameter of colony biofilms. Therefore, MP exposure seems to induce stressful conditions for colony biofilm growth and surveillance. Furthermore, MP exposure at environmental concentrations seems to change lipid distribution patterns, highlighting the complex interactions between MP and biofilm lipid composition. The redistribution of lipids towards the periphery of colonies suggests adaptive mechanisms in response to environmental stressors. Chlorine treatment significantly affected the colony biofilm architecture by changing the growth profile and roundness. The presence of both MP and chlorine exacerbated biofilm roundness perturbation, and an increase in the diameter of colony biofilms indicating an interaction between these two compounds. Therefore, current disinfection practices may need to be adjusted considering the presence of these environmental contaminants on DWDS, since biofilms sense the chemical environment and adapt their architecture accordingly. Regular monitoring of environmental contaminants in DWDS is essential to mitigate its impact on biofilm architecture and microbial community dynamics, which may have repercussions on public health since DW consumers may be exposed to microorganisms carrying critical resistance patterns. Stricter regulations on the use of parabens may also be adopted to ensure the safety and reliability of DW supplies.

Funding sources

This work was supported by Project InnovAntiBiofilm (ref. 101,157,363) financed by European Commission (Horizon-Widera 2023-Acess-02/Horizon-CSA) and national funds through FCT/MCTES (PIDDAC): LEPABE, UIDB/00511/2020 (DOI: 10.54499/UIDB/00511/2020) and UIDP/00511/2020 (DOI:10.54499/UIDP/00511/2020) and ALiCE, LA/P/0045/2020 (DOI: 10.54499/LA/P/0045/2020); Ana Rita Pereira's PhD scholarship (2021.06226.BD) and Inês B. Gomes contract 2022.06488.CEECIND/CP1733/CT0008 (DOI: 10.54499/2022.06488.CEECIND/CP1733/CT0008) both provided by FCT. Liam Rooney was funded by the Leverhume Trust. Gail McConnell was supported by the Medical Research Council [MR/K015583/1] and Biotechnology & Biological Sciences Research Council [BB/P02565X/1, BBT011602].

CRediT authorship contribution statement

Ana Rita Pereira: Writing – original draft, Methodology, Investigation, Data curation, Conceptualization. **Liam M. Rooney:** Writing – review & editing, Supervision, Data curation. **Inês B. Gomes:** Writing – review & editing, Supervision. **Manuel Simões:** Writing – review & editing, Supervision, Project administration. **Gail McConnell:** Writing – review & editing, Supervision, Resources, Project administration, Funding acquisition, Data curation.

Declaration of competing interest

The authors declare that they have no known competing financial interests or personal relationships that could have appeared to influence the work reported in this paper.

Data availability

Data will be made available on request.

Acknowledgments

The authors thank Dr. Uwe Mamat from Cellular Microbiology, Priority Research Area Infections, Research Center Borstel, Leibniz Lung Center, Borstel, Germany, for the kindly providing the *Stenotrophomonas maltophilia* UV74-sfGFP (*S. maltophilia-gfp*) strain.

Appendix A. Supplementary data

Supplementary data to this article can be found online at https://doi.org/10.1016/j.scitotenv.2024.175646.

References

Alawi, M., Smyth, C., Drissner, D., Zimmerer, A., Leupold, D., Müller, D., Do, T.T., Velasco-Torrijos, T., Walsh, F., 2024. Private and well drinking water are reservoirs for antimicrobial resistant bacteria. npj Antimicrob Resist 2, 7. https://doi.org/10.1038/s44259-024-00024-9.

Alim, D., Sircaik, S., Panwar, S.L., 2018. The significance of lipids to biofilm formation in *Candida albicans*: an emerging perspective. J Fungi. https://doi.org/10.3390/jof4040140.

Arruda, V., Simões, M., Gomes, I., 2022. The impact of synthetic musk compounds in biofilms from drinking water bacteria. J. Hazard. Mater. 129185 https://doi.org/10.1016/j.jhazmat.2022.129185.

Auld, D.B., Has, P., Mermel, L.A., 2023. Seasonality of healthcare-associated *Stenotrophomonas maltophilia*. Infect. Control Hosp. Epidemiol. 44, 1500–1501. https://doi.org/10.1017/ice.2022.280.

Barák, I., Muchová, K., 2013. The role of lipid domains in bacterial cell processes. Int. J. Mol. Sci. https://doi.org/10.3390/ijms14024050.

Benamara, H., Rihouey, C., Jouenne, T., Alexandre, S., 2011. Impact of the biofilm mode of growth on the inner membrane phospholipid composition and lipid domains in *Pseudomonas aeruginosa*. Biochim. Biophys. Acta Biomembr. 1808, 98–105. https://doi.org/10.1016/j.bbamem.2010.09.004.

Bottura, B., Rooney, L.M., Hoskisson, P.A., McConnell, G., 2022. Intra-colony channel morphology in *Escherichia coli* biofilms is governed by nutrient availability and substrate stiffness. Biofilm 4, 100084. https://doi.org/10.1016/j.bioflm.2022.100084.

Brooke, J.S., 2021. Advances in the microbiology of *Stenotrophomonas maltophilia*. Clin. Microbiol. Rev. 34, e0003019 https://doi.org/10.1128/CMR.00030-19.

Butterfield, P.W., Camper, A.K., Ellis, B.D., Jones, W.L., 2002. Chlorination of model drinking water biofilm: implications for growth and organic carbon removal. Water Res. 36, 4391–4405. https://doi.org/10.1016/s0043-1354(02)00148-3.

Cao, B., Majors, P.D., Ahmed, B., Renslow, R.S., Silvia, C.P., Shi, L., Kjelleberg, S., Fredrickson, J.K., Beyenal, H., 2012. Biofilm shows spatially stratified metabolic responses to contaminant exposure. Environ. Microbiol. 14, 2901–2910. https://doi.org/10.1111/j.1462-2920.2012.02850.x.

Chaves Simões, L., Simões, M., 2013. Biofilms in drinking water: problems and solutions. RSC Adv. 3, 2520–2533. https://doi.org/10.1039/c2ra22243d.

Chen, X., Stewart, P.S., 2000. Biofilm removal caused by chemical treatments. Water Res. 34, 4229–4233. https://doi.org/10.1016/S0043-1354(00)00187-1.

Conrad, A., Kontro, M., Keinänen, M.M., Cadoret, A., Faure, P., Mansuy-Huault, L., Block, J.C., 2003. Fatty acids of lipid fractions in extracellular polymeric substances of activated sludge flocs. Lipids 38, 1093–1105. https://doi.org/10.1007/s11745-006-1165-y.

Dubois-Brissonnet, F., Trotier, E., Briandet, R., 2016. The biofilm lifestyle involves an increase in bacterial membrane saturated fatty acids. Front. Microbiol. 7 https://doi.org/10.3389/fmicb.2016.01673.

European Commission (EU), 2011. Commission regulation (EU) No 1130/2011 of 11 november 2011 establishing a union list of food additives approved for use in food additives, food enzymes, food flavourings and nutrients. URL https://eur-lex.europa.eu/legal-content/EN/TXT/PDF/?uri=CELEX:32011R1130&from=EN (accessed 10.26.22).

European Commission (EU), 2014. Commission regulation (EU) No 1004/2014 of 18 september 2014 amending annex V to regulation /EC No 1223/2009 of the European parliament and of the council on cosmetic products. URL https://eur-lex.europa.eu

/legal-content/EN/TXT/PDF/?uri=CELEX:32014R1004&from=EN (accessed 10.26.22).
Flasiński, M., Gawryś, M., Broniatowski, M., Wydro, P., 2016. Studies on the interactions between parabens and lipid membrane components in monolayers at the air/aqueous solution interface. Biochim. Biophys. Acta Biomembr. 1858, 836–844. https://doi.org/10.1016/j.bbamem.2016.01.002.
Flasiński, M., Kowal, S., Broniatowski, M., Wydro, P., 2018. Influence of parabens on bacteria and fungi cellular membranes: studies in model two-dimensional lipid systems. J Phys ChemB 122, 2332–2340. https://doi.org/10.1021/acs.jpcb.7b10152.
Flemming, H., Wingender, J., 2010. The biofilm matrix. Nat. Rev. Microbiol. 8, 623–633 (2010). doi:https://doi.org/10.1038/nrmicro2415.
Flemming, H.-C., Percival, S.L., Walker, J.T., 2002. Contamination potential of biofilms in water distribution systems. Water Supply 2, 271–280. https://doi.org/10.2166/ws.2002.0032.
Flemming, H.-C., Wingender, J., Szewzyk, U., Steinberg, P., Rice, S.A., Kjelleberg, S., 2016. Biofilms: an emergent form of bacterial life. Nat. Rev. Microbiol. 14, 563–575. https://doi.org/10.1038/nrmicro.2016.94.
Gackowska, A., Przybyłek, M., Studziński, W., Gaca, J., 2016. Formation of chlorinated breakdown products during degradation of sunscreen agent, 2-ethylhexyl-4-methoxycinnamate in the presence of sodium hypochlorite. Environ. Sci. Pollut. Res. 23, 1886–1897. https://doi.org/10.1007/s11356-015-5444-0.
Kenchenten, K., 2017. Interaction between Micropollutants and Degradative Biofilm Communities: Basis for a Biomimetic Approach to Water Treatment.
Li, X.F., Mitch, W.A., 2018. Drinking water disinfection byproducts (DBPs) and human health effects: multidisciplinary challenges and opportunities. Environ. Sci. Technol. 52, 1681–1689. https://doi.org/10.1021/acs.est.7b05440.
Lin, H., Zhu, X., Wang, Y., Yu, X., 2017. Effect of sodium hypochlorite on typical biofilms formed in drinking water distribution systems. J. Water Health 15, 218–227. https://doi.org/10.2166/wh.2017.141.
Liu, S., Gunawan, C., Barraud, N., Rice, S.A., Harry, E.J., Amal, R., 2016. Understanding, monitoring, and controlling biofilm growth in drinking water distribution systems. Environ. Sci. Technol. https://doi.org/10.1021/acs.est.6b00835.
Liu, S., Zhang, Z., Zhao, C., Zhang, M., Han, F., Hao, J., Wang, X., Shan, X., Zhou, W., 2024. Nonlinear responses of biofilm bacteria to alkyl-chain length of parabens by DFT calculation. J. Hazard. Mater. 134460 https://doi.org/10.1016/j.jhazmat.2024.134460.
Mamat, U., Hein, M., Grella, D., Taylor, C.S., Scholzen, T., Alio, I., Streit, W.R., Huedo, P., Coves, X., Conchillo-Solé, O., Gómez, A.-C., Gibert, I., Yero, D., Schaible, U.E., 2023. Improved mini-Tn7 delivery plasmids for fluorescent labeling of *Stenotrophomonas maltophilia*. Appl. Environ. Microbiol. 89 https://doi.org/10.1128/aem.00317-23.
McConnell, G., Trägårdh, J., Amor, R., Dempster, J., Reid, E., Bradshaw Amos, W., 2016. A novel optical microscope for imaging large embryos and tissue volumes with sub-cellular resolution throughout. Elife 5. https://doi.org/10.7554/eLife.18659.001.
Nowak, K., Ratajczak-Wrona, W., Górska, M., Jabłońska, E., 2018. Parabens and their effects on the endocrine system. Mol. Cell. Endocrinol. https://doi.org/10.1016/j.mce.2018.03.014.
Pereira, A.R., Gomes, I.B., 2024. The effects of methylparaben exposure on biofilm tolerance to chlorine disinfection. J. Hazard. Mater. 134883 https://doi.org/10.1016/j.jhazmat.2024.134883.
Pereira, A.R., Gomes, I.B., Simões, M., 2023a. Impact of parabens on drinking water bacteria and their biofilms: the role of exposure time and substrate materials. J. Environ. Manag. 332, 117413 https://doi.org/10.1016/j.jenvman.2023.117413.
Pereira, A.R., Simões, M., Gomes, I.B., 2023b. Parabens as environmental contaminants of aquatic systems affecting water quality and microbial dynamics. Sci. Total Environ. https://doi.org/10.1016/j.scitotenv.2023.167332.
Postigo, C., Gil-Solsona, R., Herrera-Batista, M.F., Gago-Ferrero, P., Alygizakis, N., Ahrens, L., Wiberg, K., 2021. A step forward in the detection of byproducts of anthropogenic organic micropollutants in chlorinated water. Trends Environ Anal Chem 32, e00148. https://doi.org/10.1016/j.teac.2021.e00148.
Rivera, E.S., Weiss, A., Migas, L.G., Freiberg, J.A., Djambazova, K.V., Neumann, E.K., Van de Plas, R., Spraggins, J.M., Skaar, E.P., Caprioli, R.M., 2022. Imaging mass spectrometry reveals complex lipid distributions across *Staphylococcus aureus* biofilm layers. J Mass Spectrom Adv Clin Lab 26, 36–46. https://doi.org/10.1016/j.jmsacl.2022.09.003.
Rooney, L.M., Amos, W.B., Hoskisson, P.A., McConnell, G., 2020. Intra-colony channels in *E. Coli* function as a nutrient uptake system. ISME J. 14, 2461–2473. https://doi.org/10.1038/s41396-020-0700-9.
Schindelin, J., Arganda-Carreras, I., Frise, E., Kaynig, V., Longair, M., Pietzsch, T., Preibisch, S., Rueden, C., Saalfeld, S., Schmid, B., Tinevez, J.Y., White, D.J., Hartenstein, V., Eliceiri, K., Tomancak, P., Cardona, A., 2012. Fiji: an open-source platform for biological-image analysis. Nat. Methods. https://doi.org/10.1038/nmeth.2019.
Schniete, J., Franssen, A., Dempster, J., Bushell, T.J., Amos, W.B., McConnell, G., 2018. Fast optical sectioning for widefield fluorescence mesoscopy with the Mesolens based on HiLo microscopy. Sci. Rep. 8 https://doi.org/10.1038/s41598-018-34516-2.
Simões, L.C., Simões, M., Oliveira, R., Vieira, M.J., 2007. Potential of the adhesion of bacteria isolated from drinking water to materials. J. Basic Microbiol. 47, 174–183. https://doi.org/10.1002/jobm.200610224.
Stanton, I.C., Tipper, H.J., Chau, K., Klümper, U., Subirats, J., Murray, A.K., 2022. Does environmental exposure to pharmaceutical and personal care product residues result in the selection of antimicrobial-resistant microorganisms, and is this important in terms of human health outcomes? Environ. Toxicol. Chem. 43, 623–636. https://doi.org/10.1002/etc.5498.
Stewart, P.S., Rayner, J., Roe, F., Rees, W.M., 2001. Biofilm penetration and disinfection efficacy of alkaline hypochlorite and chlorosulfamates. J. Appl. Microbiol. 91, 525–532. https://doi.org/10.1046/j.1365-2672.2001.01413.x.
Tsvetanova, Z.G., Dimitrov, D.N., Najdenski, H.M., 2022. Prevalence of antimicrobial resistance in a Bulgarian drinking water supply system. Water Supply 22, 7059–7071. https://doi.org/10.2166/ws.2022.302.
Vandana, Priyadarshanee M., Das, S., 2023. Bacterial extracellular polymeric substances: biosynthesis and interaction with environmental pollutants. Chemosphere 332. https://doi.org/10.1016/j.chemosphere.2023.138876.
Wang, H., Hu, C., Shen, Y., Shi, B., Zhao, D., Xing, X., 2019. Response of microorganisms in biofilm to sulfadiazine and ciprofloxacin in drinking water distribution systems. Chemosphere 218, 197–204. https://doi.org/10.1016/j.chemosphere.2018.11.106.
Wang, J., Li, X., Kong, R., Wu, J., Wang, X., 2022. Fractal morphology facilitates *Bacillus subtilis* biofilm growth. Environ. Sci. Pollut. Res. 29, 56168–56177. https://doi.org/10.1007/s11356-022-19817-4.
Wang, X., Yu, D., Chen, G., Liu, C., Xu, A., Tang, Z., 2021. Effects of interactions between quorum sensing and quorum quenching on microbial aggregation characteristics in wastewater treatment: a review. Water Environ. Res. https://doi.org/10.1002/wer.1657.
Wei, F., Mortimer, M., Cheng, H., Sang, N., Guo, L.H., 2021. Parabens as chemicals of emerging concern in the environment and humans: a review. Sci. Total Environ. 778 https://doi.org/10.1016/j.scitotenv.2021.146150.
Wilking, J.N., Zaburdaev, V., De Volder, M., Losick, R., Brenner, M.P., Weitz, D.A., 2013. Liquid transport facilitated by channels in *Bacillus subtilis* biofilms. Proc. Natl. Acad. Sci. USA 110, 848–852. https://doi.org/10.1073/pnas.1216376110.
World Health Organization (WHO), 2017. Guidelines for drinking-water quality Fourth Edition Incorporating the First Addendum., 4th ed.